

1 **Evolutionary conservation and divergence of the  
2 transcriptional regulation of bivalve shell secretion across  
3 life history stages**

4 Alessandro Cavallo<sup>1,2</sup>, Melody S. Clark<sup>1</sup>, Lloyd S. Peck<sup>1</sup>, Elizabeth M. Harper<sup>3</sup> &  
5 Victoria A. Sleight<sup>1,4,5\*</sup>

6 <sup>1</sup> Biodiversity, Evolution and Adaptation Team, British Antarctic Survey, Cambridge,  
7 UK

8 <sup>2</sup> Present Address = MRC Molecular Haematology Unit, MRC Weatherall Institute of  
9 Molecular Medicine, University of Oxford, Oxford, UK

10 <sup>3</sup> Department of Earth Sciences, University of Cambridge, Cambridge, UK

11 <sup>4</sup> Department of Zoology, University of Cambridge, Cambridge, UK

12 <sup>5</sup> School of Biological Sciences, University of Aberdeen, Aberdeen, UK

13 \* Corresponding Author Victoria A. Sleight ([victoria.sleight@abdn.ac.uk](mailto:victoria.sleight@abdn.ac.uk))

14

15 **Abstract**

16 Adult molluscs produce shells with diverse morphologies and ornamentations,  
17 different colour patterns and microstructures. The larval shell however, is a  
18 phenotypically more conserved structure. How do developmental and evolutionary  
19 processes generate varying diversity at different life history stages? Using live-  
20 imaging, histology, scanning electron microscopy and transcriptomic profiling, we  
21 have described shell development in a heteroconchian bivalve the Antarctic clam,  
22 *Laternula elliptica* and compared it to adult shell secretion processes in the same  
23 species. Adult downstream shell genes, such as those encoding extracellular matrix  
24 proteins and biomineralisation enzymes, were largely not expressed during shell  
25 development, and instead, a development-specific downstream gene repertoire was  
26 expressed. Upstream regulatory genes such as transcription factors and signalling  
27 molecules were conserved between developmental and adult shell secretion.  
28 Comparing heteroconchian transcriptomic data with recently reported pteriomorphian  
29 larval shell proteome data suggests that, despite being phenotypically more conserved,  
30 the downstream effectors constituting the larval shell “tool-kit” may be as diverse as  
31 that of adults. Overall, our new data suggests that a larval shell formed using  
32 development-specific downstream effector genes is a conserved and ancestral feature  
33 of the bivalve lineage, and possibly more broadly across the molluscs.

34

35 **Introduction**

36 Molluscan shells are environmentally, economically and evolutionarily important (McDougall  
37 and Degnan 2018). The hard multifunctional external shells of molluscs are often attributed to  
38 the evolutionary success of this group. Shells are exquisitely preserved in the fossil record  
39 and their expansive extant adaptive diversity of form, as well as remarkable phenotypic  
40 plasticity, provides a powerful system to study morphological evolution (Thompson 1992). In  
41 the last decade, deciphering the molecular mechanisms that control shell secretion has  
42 received particular focus (Clark et al. 2020). A range of gastropod (Herlitze et al. 2018; Marie  
43 et al. 2010), cephalopod (Marie et al. 2009; Setiamarga et al. 2020) and bivalve (Arivalagan  
44 et al. 2017; Sleight et al. 2016a) shells have been subject to proteomic sequencing, coupled  
45 to the transcriptomic investigation of the shell-secreting mantle tissue (Arivalagan et al. 2016;  
46 Sleight et al. 2016b), resulting in large lists of candidate shell-forming genes and proteins.  
47 Comparative methods have found that despite the “deep” homology of molluscan shells and  
48 shell plates (Vinther 2015), the molecular mechanisms that control biomineralisation in  
49 molluscs – particularly the downstream effectors such as the shell matrix proteins - are  
50 extraordinarily diverse (Jackson et al. 2006). Features such as repeat low complexity domains  
51 (RLCD), domain shuffling and co-option (Aguilera et al. 2017), gene family expansions and  
52 subsequent subfunctionalisation (Aguilera et al. 2014) drive much of the observed molecular  
53 diversity. A handful of core protein domains however, are essential for all molluscan  
54 biomineralisation, regardless of morphologies, microstructures or polymorphs (carbonic  
55 anhydrase, chitin-binding, VWA and tyrosinase domains; Arivalagan et al. 2017). Due to the  
56 likelihood of fossilization, ease of study and ability to collect sufficiently large samples, there  
57 is an overwhelming bias towards adult shell studies, particularly in proteomic and  
58 transcriptomic studies. In developmental studies, some candidate gene approaches have  
59 been successfully used (Hohagen and Jackson 2013; Liu et al. 2017; 2020; Nederbragt et al.  
60 2002), but comparatively little is known about the molecular processes that pattern and  
61 generate the embryonic shell field, larval mantle and early shell secretion.

62 Phenotypically, larval mollusc shells are more conserved than adult shells in terms of  
63 morphology, crystal polymorph and microstructure; they are unsculptured simplified forms  
64 composed of an organic outer layer and aragonite mineralised layer (Weiss et al. 2002). More  
65 generally, developmental processes are highly conserved and under strong selective  
66 constraints (Prud'homme and Gompel 2010; Smith et al. 1985) and so, if there are deeply  
67 homologous molecular mechanisms directing the production of the molluscan shell, they are  
68 more likely present during developmental stages. Although limited in number and taxonomic  
69 coverage, studies on the molecular control of shell development have uncovered intriguing  
70 insights. Recent work in pteriomorphian bivalves (oysters and mussels) compared the

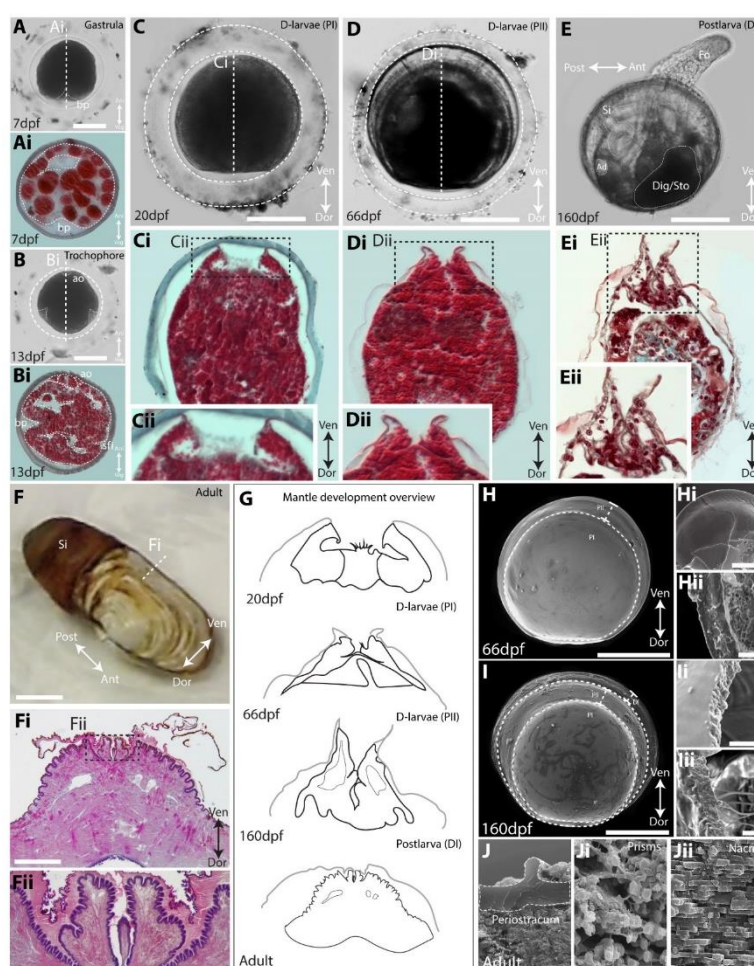
71 proteomes of larval shells to that of adults in the same species and showed that the repertoire  
72 of extracellular matrix proteins in the larval shell is almost completely different to that of the  
73 adult shell (Carini et al. 2019; Zhao et al. 2018). Only the handful of core protein domains that  
74 have been previously described as the core “tool-kit” for molluscan biomineralisation were  
75 shared between the two life history stages (carbonic anhydrase, chitin-binding and VWA). To  
76 date, intraspecific comparisons of the molecular mechanisms governing larval versus adult  
77 shell production are restricted to one bivalve infraclass (Pteriomorpha, e.g. oysters and  
78 mussels). These studies exclusively used proteomics in a qualitative presence vs absence  
79 approach, with non-replicated estimates of transcript abundance through ontogeny. They were  
80 the first studies to reveal the striking difference between larval and adult shells at the molecular  
81 level and they focus solely on the post-translationally modified downstream effectors, ie the  
82 shell matrix proteins. Much less is known about the transcriptional mechanisms that regulate  
83 early shell development, in comparison with the adult shell of the same species.  
84 Here we studied shell development using imaging and quantitative transcriptomics in a  
85 member of the Heteroconchia infraclass, the Antarctic clam, *Laternula elliptica*. Heteroconchia  
86 split from the rest of the Autobranchia in the Cambrian Period, around 500 million years ago  
87 (mya; Plazzi and Passamonti 2010), and so comparisons within the Autobranchia but between  
88 Heteroconchia and Pteriomorpha shed light on features that are deeply conserved within the  
89 bivalves over 500 million years of evolutionary time.

90

91 **Results**

92 **Morphological mantle and shell landmarks through development in *Laternula elliptica***

93 To phenotypically characterise the development of the shell field, larval mantle and shell in *L.*  
94 *elliptica*, a combination of live light imaging, histological staining and scanning electron  
95 microscopy was used (Fig. 1). Phenotypic characterisations allowed us to assign key mantle  
96 and shell landmarks to each of the development stages studied (mantle fold appearance,  
97 organic vs mineralised shell, prodissoconch I vs prodissoconch II vs dissoconch I shell) to use  
98 as a framework to decipher the transcriptional regulation of shell secretion.



99 **Figure 1. Shell and mantle development in *Laternula elliptica* characterised using live**  
100 **imaging, histology and Scanning Electron Microscopy (SEM).** **A-Ai** Invagination of the  
101 blastopore (bp) during gastrulation 7 days post fertilization (dpf) forming the archenteron prior  
102 to shell field induction (encapsulated, scale bar 60µm). **B-Bi** Early trochophore 13dpf apical  
103 organ (ao) and shell field invagination (sfi) (encapsulated, scale bar 60µm). **C-Cii** Early D-  
104 stage larvae 20dpf, first prodissoconch I organic shell (PI) secreted by unfolded larval mantle  
105 (Ci-Cii), reduced ciliary velum resorbing (Cii) (encapsulated, scale bar 60µm). **D-Dii** Late D-  
106 stage larvae 66dpf with prodissoconch II (PII) that is mineralized, mantle folds appear and  
107 fuse to form the early fused inner mantle fold (capsule disintegrating, scale bar 60µm). **E-Eii**  
108 Hatchling postlarva 166dpf with mineralised dissoconch (DI) secreted by one cell thick folded  
109 mantle (Ei-Eii), siphon (Si), adductor muscle attachment (Ad) and digestive gland/stomach  
110 (Dig/sto) are visible through the transparent shell, foot (fo) active (scale bar 100µm). **F-Fii**

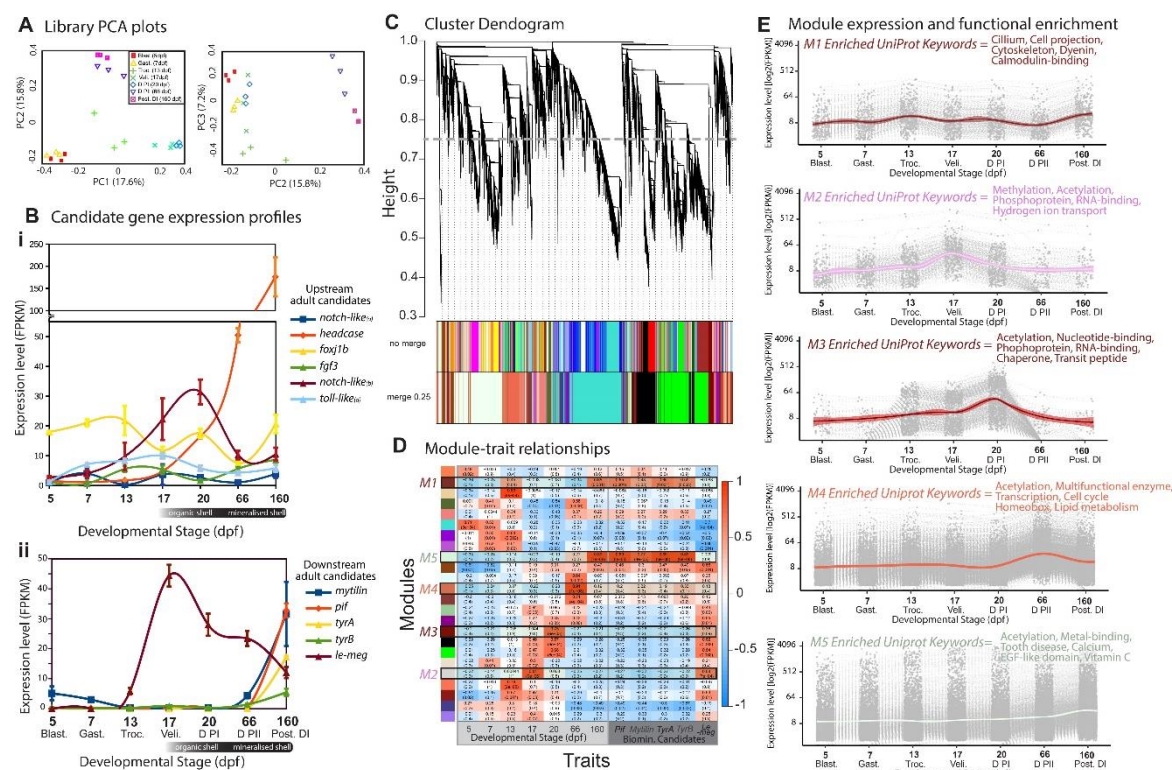
111 Adult mantle with outer folds and fused inner fold, periostracal grooves secreting two-layered  
112 periostracum, scale bar = 2mm, reproduced with permission from Sleight et al. (2016a). **G**  
113 Schematised overview of mantle morphogenesis, mantle tissue black, periostracum grey. At  
114 late D-larvae stage PII (66dpf) mineralisation coincides with formation of folds in larval mantle  
115 edge. **H-Hii** SEM of late D-larval shell 66dpf showing delineated PI and PII shells, polygonal  
116 mottling on the dorsal surface suggestive of the calcification nucleation points, Hii & Hii show  
117 the shell is brittle and hence mineralised, H scale bar 100µm, Hi scale bar 35µm, Hii scale bar  
118 10µm. **I-iii** SEM of postlarval shell 160dpf DI delineated from PI and PII shells, arenophilic  
119 secretions and intraperiostracal spikes present. I scale bar 100µm, Ii scale bar 5µm, Iii scale  
120 bar 3µm. **J-Jii** SEM cross section of adult shell microstructure, a relatively think periostracum  
121 (J), an outer layer of aragonitic granular prisms (Ji) and an inner layer of aragonitic nacreous  
122 sheets (Jii), scale bars 5µm.

123 Transcriptional characterisation of shell development in *Laternula elliptica*

124 First, a candidate gene approach was used to ask if the larval shell is built using the same  
125 protein coding genes as the adult shell. The expression of six genes encoding upstream  
126 regulatory proteins such as transcription factors and signalling molecules, and five  
127 downstream effector genes encoding extracellular matrix proteins and biomineralisation  
128 enzymes, were quantified over developmental time. All candidates had previously been  
129 characterised in adult shell secretion and repair in this species (via transcriptomics,  
130 computational gene network predictions, shell proteomics, qPCR and mRNA *in situ*  
131 hybridisations (Sleight et al. 2020; Sleight et al. 2016a; Sleight et al. 2015)). All of the upstream  
132 regulatory candidates were expressed during development, either increasing over time, or  
133 oscillating between stages (Fig. 2Bi). Only one of the downstream candidates, *le-meg*, was  
134 expressed during early shell development and the remaining four (*mytilin*, *pif*, *tyrA* and *tyrB*)  
135 were only expressed in the latest postlarva stage (Fig. 2Bii).

136 Next, genes with developmental expression profiles indicating likely involvement in regulating  
137 shell development were screened. A trait-based approach, using Weighted Correlation  
138 Network Analysis (WGCNA) was used to cluster expression profiles into modules (Fig. 2C).  
139 Module-trait relationships were then calculated to identify sets of genes (eigengenes) whose  
140 expression significantly correlated to the previously identified mantle and shell development  
141 landmarks. Five eigengene modules (M1-5) were extracted based on their significant positive  
142 correlation to traits of interest ( $P<0.001$ ,  $R>0.65$ , Fig. 2D-E). M1 contained 352 genes and  
143 was significantly positively correlated to the postlarva stage (DI, mineralised, intraperiostracal  
144 spikes and arenophilic secretions) and the average expression profile of two downstream  
145 adult candidate shell genes (*pif* and *tyrA*). M1 was enriched in genes related to the  
146 cytoskeleton, protein transport (dynein) and calmodulin-binding (conserved developmental  
147 genes in this module include: *arm*, *ltbp4*, *foxj1*, *vwa3a*, *iqcg*, *camk4*). M2 contained 337 genes  
148 whose expression profiles significantly positively correlated to veliger stage 17dpf (first organic  
149 PI initially deposited) and the average expression profile of one downstream adult candidate

150 gene (*le-meg*). M2 was enriched in genes related to methylation and hydrogen ion transport  
 151 (conserved developmental genes in this module include: *alpl*, *chs2*, *sbp1*, *h2b*). M3 contained  
 152 647 genes and was significantly positively correlated to early D-larvae (PI) stage 20dpf (first  
 153 organic shell) but none of the adult candidate shell genes. M3 was enriched in genes related  
 154 to protein folding and protein transport (conserved developmental genes in this module  
 155 include: *hsp70*, *cpn601*, *hsp90*, *btf3*, *ccb23*). M4 contained 2,875 genes whose expression  
 156 significantly positively correlated to late D-larvae (PII) stage 66dpf (mineralised shell) but none  
 157 of the adult candidate shell genes. M4 was enriched in genes related to proliferation/growth,  
 158 hox code transcription factors and multi-functional enzymes (conserved developmental genes  
 159 in this module include: *a-somp*, *fgf1*, *abd-a*, *abd-b*, *nkx2.6*, *mox1*). M5 contained 6,369 genes  
 160 significantly positively correlated to postlarva stage (DI) 160dpf and the average expression  
 161 profile of four of the adult biomimetication candidate genes (*pif*, *mytilin*, *tyrA* and *tyrB*). M5  
 162 was enriched in genes related to calcification, egf-like domains and vitamin C (conserved  
 163 developmental genes in this module include: *bmp2*, *bmp3*, *bmp7*, *fgf1-1*, *ca*, *fz4*, *notch1*, *wnt4*,  
 164 *wnt2b*, *tyr2*, *perl*). Modules 2-4 contain genes whose expression dynamics suggest they are  
 165 involved in the regulation of early larval shell, whereas M1 and M5 are both correlated to the  
 166 downstream adult shell genes and show an increase in expression only in the latest stage, the  
 167 postlarva (Supplementary file 1).



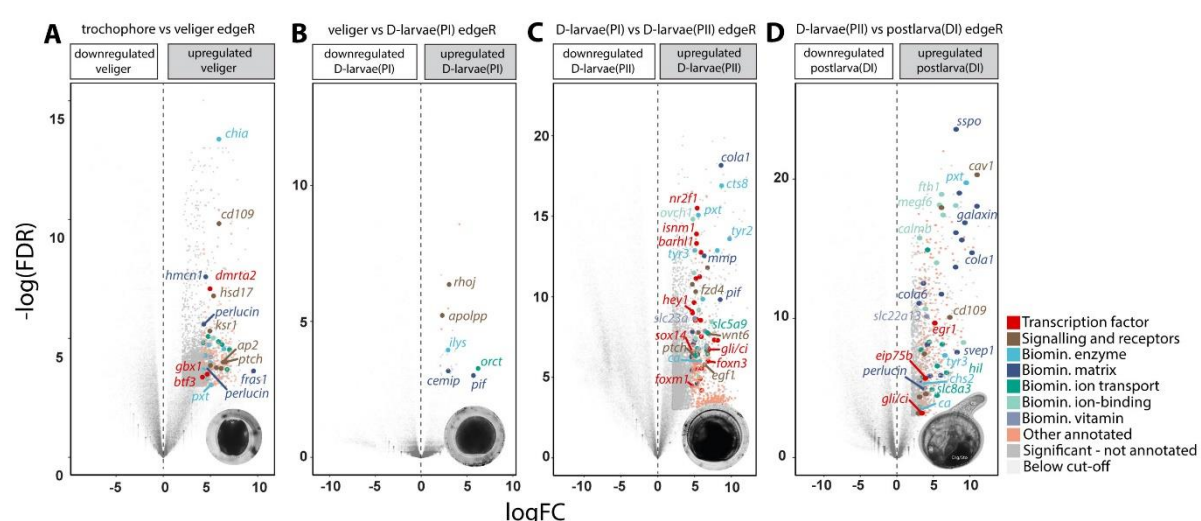
168 **Figure 2. Candidate gene and trait-based approach to decipher transcriptional  
 169 regulation of mantle and shell development in *Laternula elliptica* using bulk RNA-Seq.**  
 170 A PCA plots (PC1-3) of each RNA-seq library clustering by developmental stage (n=3 libraries

171 per stage). **B** Average expression (Fragments Per Kilobase of transcript per Million [FPKM],  
172 mean average, +/- S.E., n=3) at each stage of shell development of candidate upstream  
173 regulatory and downstream effector genes. **C** Dendrogram obtained by average linkage  
174 hierarchical clustering using the Weighted Correlation Network Analysis (WGCNA) R  
175 package, module assignment determined by the Dynamic Tree Cut after merging at 75% cut-  
176 off. **D** Correlation of eigengene modules to shell development traits (dpf and expression of  
177 candidate downstream adult biomineralisation genes). Each row corresponds to an eigengene  
178 module and each column a trait, color-coded by direction and degree of the correlation  
179 (Pearson R, red = positive correlation; blue = negative correlation). Five eigengene modules  
180 are highlighted (M1-M5) as they significantly positively correlate to shell development traits of  
181 interest. **E** All transcripts in each eigengene module of interest (M1-M5) extracted and mean  
182 average FPKM plotted over developmental time (n=3, shaded +/- 95% confidence interval,  
183 method = loess). Selected biologically interesting significantly enriched Uniprot keywords  
184 highlighted (calculated using String-DB, supplementary file 1).

185

186 A second unbiased statistical approach was used to identify genes that were upregulated at  
187 each consecutive stage of shell development. Significantly upregulated genes were screened  
188 for functional categories relating to shell secretion (Fig. 3), extracted, and plotted over time in  
189 clustered heatplots (Fig. S1). Genes upregulated at the D-larvae (PII) stage included a striking  
190 number of transcription factors and signalling molecules, such as components of the hh and  
191 wnt signalling pathways (*gli*, *ptch*, *fzd4* and *wnt6*). The stage that had the fewest upregulated  
192 genes was D-larvae (PI) with 25 genes upregulated including genes involved in signalling (*rhol*  
193 and *apolpp*), ion transport (*orct*) and the extracellular shell matrix (*pif*) (Supplementary file 1).  
194 Many of the screened biomineralisation genes had a stage-specific expression pattern. For  
195 example, genes that were highly upregulated in the postlarva stage (when the downstream  
196 adult shell candidates are also highly expressed) were expressed at very low levels through  
197 all of the earlier stages of shell development. Some of the stage-specific expression patterns  
198 were explained by ontogenetic partitioning of isoforms and/or paralogues (indicated with  
199 arrows Fig. S1), for example we found an isoform of *ptch3* that was expressed only in early  
200 shell development (significantly upregulated in the veliger stage) and a different isoform only  
201 expressed late in shell development (significantly upregulated in D-larvae PII stage).

202



203 **Figure 3. Unbiased pairwise differential expression approach to decipher**  
204 **transcriptional regulation of shell development in *Laternula elliptica*.** Differential  
205 expression was determined using edgeR with a negative binomial additive general linear  
206 model and quasi-likelihood F-test, corrected for multiple testing using the Benjamin-Hochberg  
207 method to control the false discovery rate (FDR). Upregulated genes at each stage screened  
208 for statistical significance (FDR<0.05), magnitude ( $\log_2\text{FC}>2$ ) and functional categories related  
209 to shell development, as per colour-coded key. Specific genes of biological interest are  
210 labelled. **A** upregulated genes at initial organic shell stage, veliger 17dpf. **B** upregulated genes  
211 at early D-larvae (PI) stage 20dpf with full organic PI shell. **C** upregulated genes at late D-  
212 larvae (PII) stage 66dpf when larval shell first begins to be mineralised and folds established  
213 in the larval mantle. **D** upregulated genes in hatchling postlarva (DI) stage 160dpf.

214

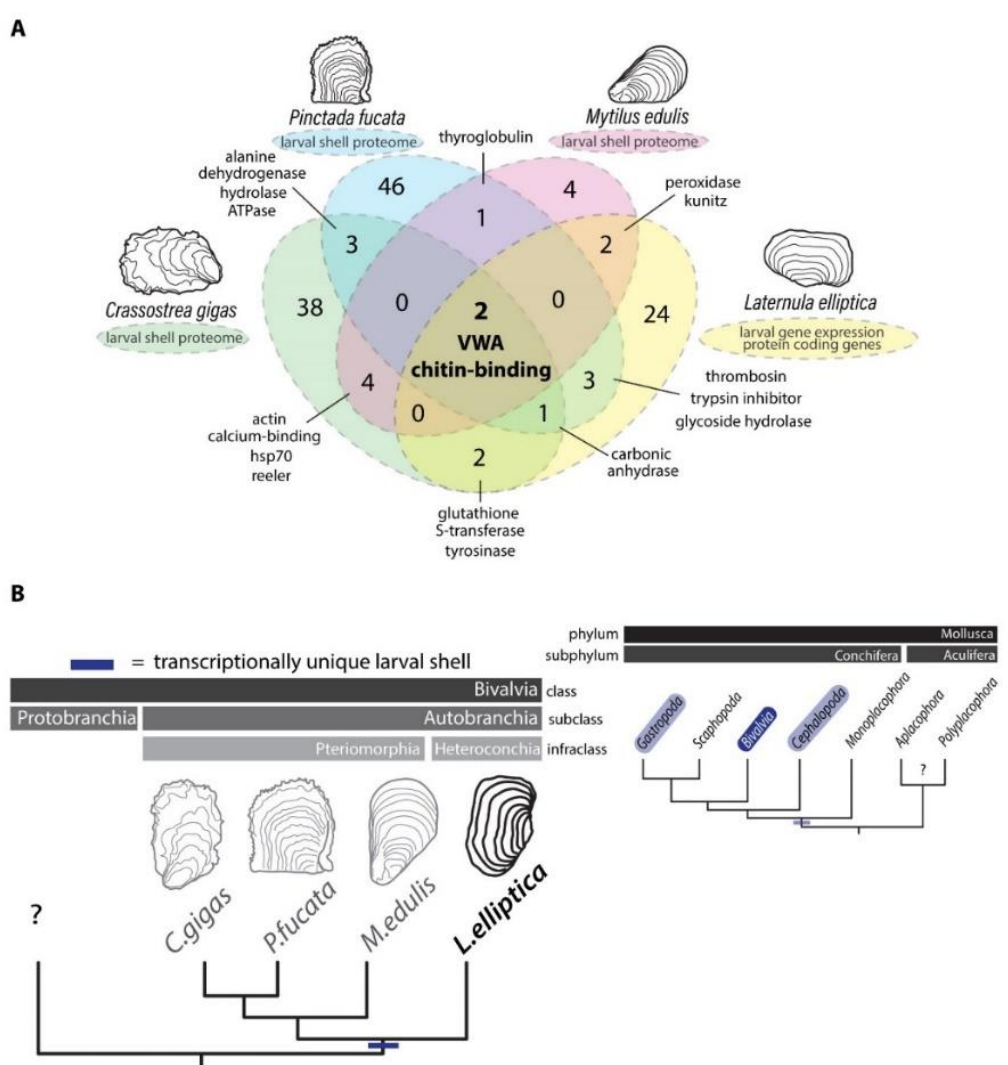
215 The signalling components upregulated during the shell development stages include hh and  
216 wnt pathways (Fig. 4A-B). To further explore the possible role of these signalling pathways in  
217 shell development we extracted genes relating to the canonical transduction of the hh and wnt  
218 pathways and plotted them over developmental time (Fig. S2). Most of the hh and wnt  
219 signalling genes were expressed prior to the secretion of the larval shell, followed by very low  
220 levels during early shell development stages— veliger and D larvae (PI) stages. One exception  
221 was a *ptch* isoform, which was upregulated again at the late D (PII) stage, coinciding with the  
222 beginning of larval mantle folding and onset of mineralisation.

223

#### 224 Interspecies comparison of the molecular control of larval shell development

225 To test if larval shell matrix proteins are more conserved than those of adults, genes identified  
226 as likely larval shell downstream effectors in *L. elliptica* were compared with the three publicly  
227 available larval shell proteomes (*Crassostrea gigas*, *Pinctada fucata* and *Mytilus edulis*).  
228 Protein domains were compared across the four species to search for conserved vs lineage

229 specific domains, as per Arivalagan et al. (2017). Only two protein domains were present in all  
230 four species larval shell datasets, VWA and chitin-binding, carbonic anhydrase was present  
231 in three out of four species (Fig. 4A).



254 **Figure 4. Development-specific downstream effectors control larval shell production in**  
255 **autobranchians, and more broadly across conchiferans. A** Larval downstream effectors,  
256 such as shell matrix proteins and biominerallisation enzymes translated to amino acid  
257 sequences and surveyed for known domains. Protein domains compared against larval shell  
258 proteomes to search for conserved vs lineage specific domains using OrthoVenn2. **B** A  
259 development-specific larval shell proteome (versus adult shell proteome) in three species of  
260 Pteriomorphia and, presented here, transcriptionally unique, development-specific  
261 downstream shell genes in a representative from Heteroconchia points to an ancestral  
262 condition to the Autobranchia subclass. Development-specific shell genes and isoforms have  
263 also been reported in gastropods. Taken together with many conchiferan molluscs retaining a  
264 larval shell but secondarily loosing, or reducing, an adult shell leads us to hypothesise that a  
265 transcriptionally unique larval shell is likely a deeply conserved trait to the Conchifera (no  
266 known developmental data for Aculifera or Protobranchia).

267

268

269 **Discussion**

270 We have quantified the ontogenetic expression dynamics of genes putatively involved in shell  
271 development for the first time in a heteroconchian bivalve, the Antarctic clam *L. elliptica*. These  
272 genes can be broadly categorised into two groups: downstream effectors that code for proteins  
273 involved in the extracellular shell matrix, enzymes and ion transporters (such as peroxidases,  
274 chitinases, matrix metalloproteinases, galaxins, ion and vitamin transporters) and upstream  
275 regulatory genes that code for transcription factors and signalling components (wnt and hh  
276 signalling components, hox, fox and sox transcription factors). Owing to a lack of genetically  
277 tractable model systems to conduct gene function experiments in molluscs (and more broadly  
278 spiraliens), data on the gene regulatory networks that drive processes such as shell  
279 development and biomineralisation in this group are sparse, either focussing on two or three  
280 candidates (Kin et al. 2009; Liu et al. 2017; 2020; Nederbragt et al. 2002; Samadi and Steiner  
281 2009; Tan et al. 2018), or use only computational methods (Sleight et al. 2020). Previous work  
282 has implicated bmp signalling in the regulation of molluscan shell secretion using *in situ*  
283 expression data and perturbations such as RNAi, DMH1 (a bmp inhibitor) or addition of bmp  
284 protein. Results have been variable; work in bivalves suggest bmp signalling could play a role  
285 in controlling adult shell secretion (Zhao et al. 2016) and shell development (Liu et al. 2020;  
286 Nederbragt et al. 2002). More recent experiments in the gastropod *Crepidula fornicata* found  
287 that when bmp signalling was disrupted during development, there was no observed effect on  
288 shell phenotype (Lyons et al. 2020) and single-cell RNAseq data from the trochophore stage  
289 of the heteroconchian bivalve *Dreissena rostriformis* suggests no bmp gene expression in  
290 shell-field cells (Salamanca-Díaz et al. 2022). The WGCNA analysis presented here found  
291 bmp pathway components were correlated only to the postlarva stage and the upregulation of  
292 the downstream adult shell candidates, but no bmp components were found using the  
293 differential expression approach. Taken together with previous reports in other groups, we  
294 hypothesise that bmp signalling is not involved in early shell development in heteroconchian  
295 bivalves, but could play a role in controlling the growth and maintenance of shell secretion at  
296 later stages.

297 The transcriptomic profiling data presented here suggests that hh and wnt signalling pathways  
298 are involved in shell development. These signalling pathways have well characterised roles in  
299 animal dorsal-ventral (wnt) and anterior-posterior patterning (hh), and the outgrowth of  
300 appendages in vertebrates and arthropods, as well as osteoblast differentiation and digit  
301 patterning in vertebrate endoskeletons (Hiscock et al. 2017; Riddle et al. 1993; Witte et al.  
302 2009). Previous work has linked wnt signalling genes to biomineralisation in bivalves (Gao et  
303 al. 2016), and most recently, wnt and hh signalling have been shown to pattern cephalopod  
304 arm development (Tarazona et al. 2019). If cephalopod “limbs” evolved by parallel activation

305 of a gene regulatory network for appendage development that was present in the bilaterian  
306 common ancestor (Tarazona et al. 2019), our data also suggest that this genetic program for  
307 appendage development may have been co-opted for shell development. More data is  
308 required on the spatial expression and function of hh and wnt genes in relation to mollusc shell  
309 development, and future work in species more suited to such methods should prioritise these  
310 studies.

311 Recent larval shell proteomes of three pteriomorphian bivalve species report that a  
312 development-specific repertoire of downstream effector proteins are found in the extracellular  
313 matrix of the larval shell when compared to the adult shell (Carini et al. 2019; Zhao et al. 2018).  
314 Here, we asked if this pattern holds true in a heteroconchian representative, and aimed to  
315 understand the transcriptional regulation of larval shell deposition versus that of adults. We  
316 find that previously characterised downstream adult shell genes are largely not involved in  
317 larval shell secretion (except for *le-meg*), neither the first organic stage nor early mineralised  
318 stages, but that the upstream regulatory genes, such as signalling molecules and transcription  
319 factors, are more conserved between life history stages. Our data suggest that global  
320 transcriptional mechanisms underpinning the unique larval shell proteins include ontogenetic  
321 partitioning of isoforms and paralogues, in addition to some *bona fide* unique larval genes  
322 (such as *btf3*, *pap18*, *chid1*, *cemip* and *nsf*). We hypothesise that, similar to other  
323 developmental systems, such as *svb*-driven gene regulatory networks in the formation of  
324 diverse actin rich projections in arthropods (Smith et al. 2018), conserved gene regulatory  
325 networks drive shell deposition in larval and adult life history stages, but the downstream  
326 effectors activated by the network depends on local factors in different life history and cellular  
327 contexts. As is the case with many systems studying morphological evolution, questions  
328 regarding the connection between gene regulatory networks and downstream effectors, the  
329 generation of temporal and local contexts and how different downstream effectors exert  
330 influences on phenotypic outcomes, remain unanswered.

331 Terminal downstream effectors in adult shells, such as extracellular shell matrix proteins, are  
332 rapidly evolving, lineage-specific and surprisingly diverse, with just four domains critical for all  
333 molluscan biomineralisation (carbonic anhydrase, chitin-binding, VWA and tyrosinase  
334 (Arivalagan et al. 2017)). To test if this pattern holds true for early life history stages where,  
335 phenotypically at least, shells are more conserved between species, we carried out  
336 comparative domain analysis between heteroconchian and pteriomorphian bivalves. Similar  
337 to the pattern in adult life history stages for these groups, we find only two domains shared  
338 between the four species (chitin-binding and VWA domains), despite the similarity in shell  
339 phenotype across species at this stage. In our analysis we compared data generated by  
340 different groups using different methods, in addition, our data is a prediction of

341 biomineralisation effectors and hence, it is likely that the number of conserved domains are  
342 underestimated. For example, it is unlikely that carbonic anhydrase is truly absent in larval  
343 mussel shells as reported Carini et al., (2019), but rather it was technologically difficult to  
344 detect all proteins present in larval shell with the small input material that is available from  
345 developmental stages.

346 For the first time, we have compared the transcriptional regulation of shell secretion at different  
347 life history stages of a heteroconchian bivalve. Studying a heteroconchian representative, and  
348 comparing it to data available for pteriomorphians allows us to hypothesise that a development-  
349 specific transcriptionally unique larval shell is likely an ancestral feature of autibranchians, or  
350 perhaps even more broadly to conchiferans (Fig. 5B). Ontogenetic partitioning of some  
351 specific shell gene isoforms has been reported in gastropods, as well as alternative splicing  
352 to generate diverse shell matrix proteins from a single genomic loci (*Halitosis asinine* and  
353 *Lymnaea stagnalis* (Herlitze et al. 2018; Jackson et al. 2006)). In addition, some conchiferan  
354 molluscs have a larval shell but have secondarily lost, or reduced, an adult shell (Knutson et  
355 al. 2020). There is a huge diversity of form and function between different life history stages  
356 in molluscs. Taken together, these findings lead us to hypothesise that a development-specific  
357 transcriptionally unique larval shell may be a deeply conserved trait to the Conchifera, but  
358 more data from diverse taxa, especially the Acuifera, are needed to resolve questions on the  
359 evolution of biomimetication in the molluscs.

360

361 **Methods**

362 **Animal husbandry, spawning and developmental staging**

363 Embryos were obtained from an adult broodstock of sexually mature *L. elliptica* individuals  
364 and divided into three independent closed-system 1L tanks. Embryos were maintained at 0°C  
365 ± 0.5°C, aerated with an airstone with 50% water changes every two days using autoclaved  
366 seawater. Embryos were staged as per Peck et al. (2007).

367 **Fixation, histology and imaging**

368 For histology and Scanning Electron Microscopy (SEM), embryos were fixed in 500 µL of 2.5%  
369 glutaraldehyde in phosphate buffered saline (PBS) at room temperature for 30 minutes, rinsed  
370 twice in PBS with 0.1% tween, dehydrated into 100% ethanol and stored at 4°C.

371 For histology, embryos were cleared in Histosol (National Diagnostics, 3 × 20 min, room  
372 temperature), transitioned through 1:1 Histosol:molten paraffin (2 × 30 mins, 60°C) then pure  
373 molten paraffin (RA Lamb Wax – Fisher Scientific, 60°C overnight). Five changes of molten  
374 paraffin (each >1 hr) were conducted before embedding in a Peel-A-Way embedding mold  
375 (Sigma). Wax blocks were serially sectioned at 8 µm on a Leica RM2125 rotary microtome.  
376 Sections were stained with a modified Masson's trichrome stain as per Witten and Hall (2003).  
377 All histology was conducted on a minimum of 3 individuals per stage. Sections were imaged  
378 on a Zeiss Axioscope A1 with Zen software (at the University of Cambridge).

379 For SEM of the shell late D (66dpf) and postlarval (160dpf) stages, larvae were transferred  
380 from ethanol to electron microscope stubs, attached using carbon adhesive discs, carbon  
381 coated and examined using a QEMSCAN 650F (at the University of Cambridge) at  
382 accelerating voltages of 10 kV.

383 Each stage was also live imaged on an upright compound light microscope fitted with a camera  
384 (Olympus BX50 microscope fitted with Olympus PM-C35 camera using Olympus U-CMAD-2  
385 software, at the British Antarctic Survey) by mounting in seawater onto a glass slide, under a  
386 coverslip on small clay feet. All live imaging was conducted on a minimum of 3 individuals per  
387 stage.

388 Images were adjusted for contrast and brightness, cropped, rotated, and flipped. All plates  
389 were constructed in Adobe Illustrator software.

390 **Sampling, RNA extraction and sequencing**

391 Triplicate RNA-Seq samples were collected for each developmental stage, one from each  
392 independent tank. For each sample, exactly two hundred staged-matched embryos were snap  
393 frozen in a 70% ethanol dry ice slurry and stored at -80°C. Total RNA was extracted from each  
394 sample as per manufactures recommendations (Relia Miniprep kit, Promega) and tested for

395 quality and quantity using Nanodrop and Agilent Tapestation. All samples had an RNA  
396 Integrity Number (RIN) of over 7. Libraries were prepared by the DNA sequencing facility in  
397 the Biochemistry Department at the University of Cambridge (TruSeq Stranded mRNA,  
398 Illumina) and sequenced on an Illumina NextSeq500 generating over 300 million 150bp  
399 stranded paired-end reads. All raw data is publicly available from NCBI SRA accession  
400 number: PRJNA803976.

401 **Bioinformatics and statistical analyses**

402 Raw reads (total 309,593,642) were cleaned using ea-utils tool v1.1.2 fastq-mcf (quality –q  
403 30, and length –l 100), after cleaning 296,480,254 reads remained. Prior to *de novo* assembly,  
404 reads were normalised using the Trinity v.2.2.0 utility script (insilico\_read\_normalization.pl –  
405 max\_cov 50), leaving 64,355,068 reads for assembly. Clean, normalised reads were  
406 assembled using Trinity v.2.2.0 with default parameters (Grabherr et al. 2011; Haas et al.  
407 2013). Assembly quality was assessed using Trinity utilities and the gVolante webserver tool  
408 (Table S1). Transcript abundance was estimated by alignment-based quantification using  
409 Trinity v.2.2.0 utilities. Transcripts from each cleaned library were aligned to the transcriptome  
410 using bowtie2 with default parameters and transcript abundance estimates were calculated  
411 using RNA-Seq by Expectation-Maximization (RSEM). Raw counts and Trimmed Mean of M-  
412 values [TMM] normalised Fragments Per Kilobase Of Exon Per Million Fragments Mapped  
413 [FPKM] matrices were generated.

414 Weighted correlation network analysis (WGCNA) was used to find clusters, termed modules,  
415 of genes with highly correlated expression across all libraries. Each cluster was then  
416 correlated to external traits of interest (Langfelder and Horvath 2008). The raw counts matrix  
417 was loaded in R and EdgeR (Robinson et al. 2010) functions were used to remove lowly  
418 expressed transcripts (keep transcripts with cpm >5 in ≥4 libraries) leaving 37,000 transcripts  
419 for WGCNA. TMM-FPKM values were used to calculate a gene dissimilarity matrix  
420 (adjacency= softpower 16 and signed, TOMsimilarity = signed) and hierarchical clustering was  
421 performed (method = average). Modules were determined using the cutreeDynamic function  
422 with a minimum gene membership threshold of 30 and dynamic tree cut-off of 25. Modules  
423 were correlated to external traits (days post fertilization or average candidate gene expression  
424 values). Modules of that were significantly correlated to traits of interest were extracted and  
425 all transcripts were putatively annotated based on sequence similarity searched using blastx  
426 against Uniprot (<http://www.uniprot.org/>), and tested for functional enrichment.

427 Pairwise differential gene expression tests were performed to find transcripts that were  
428 upregulated at each stage of shell development (compared to the previous stage). Using the  
429 EdgeR package, a negative binomial additive general linear model with a quasi-likelihood F-

430 test was performed and p-values were adjusted for multiple testing using the Benjamini-  
431 Hochberg method to control the false discovery rate, cut-offs for statistical significance (FDR  
432  $\leq 0.05$ ) and magnitude were used ( $\log_2\text{FC}>2$ ). Upregulated transcripts were putatively  
433 annotated based on sequence similarity searched using blastx against Uniprot  
434 (<http://www.uniprot.org/>), and screened for functional categories relating to gene regulation  
435 and shell secretion.

436 All upregulated genes that were functionally categorised as downstream effectors, such as  
437 shell matrix proteins and biomineralisation enzymes were translated to amino acid sequences  
438 and surveyed for known domains. Protein domains were then compared against published  
439 larval shell proteomes for oyster (Zhao et al. 2018) and mussel (Carini et al. 2019) species to  
440 search for conserved vs lineage specific domains as per Arivalagan et al., (2017), using  
441 OrthoVenn2.

442

443 **References**

444 Aguilera F, McDougall C, Degnan BM. 2014. Evolution of the tyrosinase gene family in bivalve  
445 molluscs: Independent expansion of the mantle gene repertoire. *Acta biomaterialia*.  
446 10(9):3855-3865.

447 Aguilera F, McDougall C, Degnan BM. 2017. Co-option and de novo gene evolution underlie  
448 molluscan shell diversity. *Mol Biol Evol*. 34(4):779-792.

449 Anishchenko E, Arnone MI, D'Aniello S. 2018. In sea urchin development: Implications in  
450 neurogenesis, ciliogenesis and skeletal patterning. *Evodevo*. 9:5.

451 Arivalagan J, Marie B, Sleight VA, Clark MS, Berland S, Marie A. 2016. Shell matrix proteins  
452 of the clam, *Mya truncata*: Roles beyond shell formation through proteomic study.  
453 *Marine Genomics*. 27:69-74.

454 Arivalagan J, Yarra T, Marie B, Sleight VA, Duvernois-Berthet E, Clark MS, Marie A, Berland  
455 S. 2017. Insights from the shell proteome: Biomineralization to adaptation. *Mol Biol  
456 Evol*. 34(1):66-77.

457 Carini A, Koudelka T, Tholey A, Appel E, Gorb SN, Melzner F, Ramesh K. 2019. Proteomic  
458 investigation of the blue mussel larval shell organic matrix. *J Struct Biol*.  
459 208(3):107385.

460 Clark MS, Peck LS, Arivalagan J, Backeljau T, Berland S, Cardoso JCR, Caurcel C, Chapelle  
461 G, De Noia M, Dupont S et al. 2020. Deciphering mollusc shell production: The roles  
462 of genetic mechanisms through to ecology, aquaculture and biomimetics. *Biol Rev Camb Philos Soc*. 95(6):1812-1837.

463 Gao J, Liu J, Yang Y, Liang J, Xie J, Li S, Zheng G, Xie L, Zhang R. 2016. Identification and  
464 expression characterization of three wnt signaling genes in pearl oyster (*Pinctada  
465 fucata*). *Comp Biochem Physiol B Biochem Mol Biol*. 196-197:92-101.

466 Grabherr MG, Haas BJ, Yassour M, Levin JZ, Thompson DA, Amit I, Adiconis X, Fan L,  
467 Raychowdhury R, Zeng QD et al. 2011. Full-length transcriptome assembly from rna-  
468 seq data without a reference genome. *Nature Biotechnology*. 29(7):644-U130.

469 Haas BJ, Papanicolaou A, Yassour M, Grabherr M, Blood PD, Bowden J, Couger MB, Eccles  
470 D, Li B, Lieber M et al. 2013. De novo transcript sequence reconstruction from rna-  
471 seq: Reference generation and analysis with trinity. *Nature protocols*.  
472 8(8):10.1038/nprot.2013.1084.

473 Herlitze I, Marie B, Marin F, Jackson DJ. 2018. Molecular modularity and asymmetry of the  
474 molluscan mantle revealed by a gene expression atlas. *Gigascience*. 7(6).

475 Hiscock TW, Tschopp P, Tabin CJ. 2017. On the formation of digits and joints during limb  
476 development. *Dev Cell*. 41(5):459-465.

477 Hohagen J, Jackson DJ. 2013. An ancient process in a modern mollusc: Early development  
478 of the shell in *Lymnaea stagnalis*. *BMC Developmental Biology*. 13:13.

479 Huan P, Wang Q, Tan S, Liu B. 2020. Dorsal-ventral decoupling of hox gene expression  
480 underpins the diversification of molluscs. *Proc Natl Acad Sci U S A*. 117(1):503-512.

481 Jackson DJ, McDougall C, Green K, Simpson F, Woerheide G, Degnan BM. 2006. A rapidly  
482 evolving secretome builds and patterns a sea shell. *BMC Biology*. 4.

483 Kin K, Kakoi S, Wada H. 2009. A novel role for dpp in the shaping of bivalve shells revealed  
484 in a conserved molluscan developmental program. *Dev Biol*. 329(1):152-166.

485 Knutson VL, Brenzinger B, Schrödl M, Wilson NG, Giribet G. 2020. Most cephalaspidea have  
486 a shell, but transcriptomes can provide them with a backbone (gastropoda:  
487 Heterobranchia). *Mol Phylogenetic Evol*. 153:106943.

488 Langfelder P, Horvath S. 2008. Wgcna: An r package for weighted correlation network  
489 analysis. *BMC Bioinformatics*. 9:559.

490 Lefebvre V. 2019. Roles and regulation of sox transcription factors in skeletogenesis. *Curr  
491 Top Dev Biol*. 133:171-193.

492 Liu G, Huan P, Liu B. 2017. A soxc gene related to larval shell development and co-expression  
493 analysis of different shell formation genes in early larvae of oyster. *Dev Genes Evol*.  
494 227(3):181-188.

495

496 Liu G, Huan P, Liu B. 2020. Identification of three cell populations from the shell gland of a  
497 bivalve mollusc. *Dev Genes Evol.* 230(1):39-45.

498 Lyons DC, Perry KJ, Batzel G, Henry JQ. 2020. Bmp signaling plays a role in anterior-  
499 neural/head development, but not organizer activity, in the gastropod *crepidula*  
500 *fornicata*. *Dev Biol.* 463(2):135-157.

501 Marie B, Marie A, Jackson DJ, Dubost L, Degnan BM, Milet C, Marin F. 2010. Proteomic  
502 analysis of the organic matrix of the abalone *Haliotis asinina* calcified shell. *Proteome*  
503 *Science.* 8.

504 Marie B, Marin F, Marie A, Bédouet L, Dubost L, Alcaraz G, Milet C, Luquet G. 2009. Evolution  
505 of nacre: Biochemistry and proteomics of the shell organic matrix of the cephalopod  
506 *Nautilus macromphalus*. *Chembiochem.* 10(9):1495-1506.

507 McDougall C, Degnan BM. 2018. The evolution of mollusc shells. *Wiley Interdiscip Rev Dev*  
508 *Biol.* 7(3):e313.

509 Nederbragt AJ, van Loon AE, Dictus WJ. 2002. Expression of *Patella vulgata* orthologs of  
510 engrailed and dpp-bmp2/4 in adjacent domains during molluscan shell development  
511 suggests a conserved compartment boundary mechanism. *Dev Biol.* 246(2):341-355.

512 Plazzi F, Passamonti M. 2010. Towards a molecular phylogeny of Mollusks: Bivalves' early  
513 evolution as revealed by mitochondrial genes. *Molecular Phylogenetics and Evolution,*  
514 57(2):641-657.

515 Peck LS, Powell DK, Tyler PA. 2007. Very slow development in two antarctic bivalve molluscs,  
516 the infaunal clam *Laternula elliptica* and the scallop *Adamussium colbecki*. *Marine*  
517 *Biology.* 150(6):1191-1197.

518 Perry KJ, Lyons DC, Truchado-Garcia M, Fischer AH, Helfrich LW, Johansson KB, Diamond  
519 JC, Grande C, Henry JQ. 2015. Deployment of regulatory genes during gastrulation  
520 and germ layer specification in a model spiralian mollusc *Crepidula*. *Dev Dyn.*  
521 244(10):1215-1248.

522 Prud'homme B, Gompel N. 2010. Evolutionary biology: Genomic hourglass. *Nature.*  
523 468(7325):768-769.

524 Riddle RD, Johnson RL, Laufer E, Tabin C. 1993. Sonic hedgehog mediates the polarizing  
525 activity of the zpa. *Cell.* 75(7):1401-1416.

526 Robinson MD, McCarthy DJ, Smyth GK. 2010. Edger: A bioconductor package for differential  
527 expression analysis of digital gene expression data. *Bioinformatics.* 26(1):139-140.

528 Salamanca-Díaz DA, Schulreich SM, Cole AG, Wanninger A. 2022. Single-Cell RNA  
529 Sequencing Atlas From a Bivalve Larva Enhances Classical Cell Lineage Studies.  
530 *Front Ecol Evol.* 9:783984.

531 Samadi L, Steiner G. 2010. Expression of hox genes during the larval development of the  
532 snail, *Gibbula varia* (L.)-further evidence of non-colinearity in molluscs. *Dev Genes*  
533 *Evol.* 220(5-6):161-172.

534 Setiamarga DHE, Hirota K, Yoshida M-a, Takeda Y, Kito K, Shimizu K, Isowa Y, Ikeo K, Sasaki  
535 T, Endo K. 2020. Hydrophilic shell matrix proteins of *Nautilus pompilius* and the  
536 identification of a core set of conchiferan domains. *bioRxiv.2020.2011.2014.382804.*

537 Sleight VA, Antczak P, Falciani F, Clark MS. 2020. Computationally predicted gene regulatory  
538 networks in molluscan biomineralization identify extracellular matrix production and ion  
539 transportation pathways. *Bioinformatics.* 36(5):1326-1332.

540 Sleight VA, Marie B, Jackson DJ, Dyrynda EA, Marie A, Clark MS. 2016a. An antarctic  
541 molluscan biomineralisation tool-kit. *Sci Rep.* 6:36978.

542 Sleight VA, Thorne MA, Peck LS, Clark MS. 2015. Transcriptomic response to shell damage  
543 in the antarctic clam, *laternula elliptica*: Time scales and spatial localisation. *Mar*  
544 *Genomics.* 20:45-55.

545 Sleight VA, Thorne MAS, Peck LS, Arivalagan J, Berland S, Marie A, Clark MS. 2016b.  
546 Characterisation of the mantle transcriptome and biomineralisation genes in the blunt-  
547 gaper clam, *Mya truncata*. *Marine Genomics.* 27:47-55.

548 Smith JM, Burian R, Kauffman S, Alberch P, Campbell J, Goodwin B, Lande R, Raup D,  
549 Wolpert L. 1985. Developmental constraints and evolution: A perspective from the

550 mountain lake conference on development and evolution. *The Quarterly Review of*  
551 *Biology*. 60(3):265-287.

552 Smith SJ, Rebeiz M, Davidson L. 2018. From pattern to process: Studies at the interface of  
553 gene regulatory networks, morphogenesis, and evolution. *Curr Opin Genet Dev*.  
554 51:103-110.

555 Tan S, Huan P, Liu B. 2018. An investigation of oyster tgf- $\beta$  receptor genes and their potential  
556 roles in early molluscan development. *Gene*. 663:65-71.

557 Tarazona OA, Lopez DH, Slota LA, Cohn MJ. 2019. Evolution of limb development in  
558 cephalopod mollusks. *Elife*. 8:e43828.

559 Thompson DAW. 1992. On growth and form. Bonner JT, editor. Cambridge: Cambridge  
560 University Press.

561 Vinther J. 2015. The origins of molluscs. *Palaeontology*. 58(1):19-34.

562 Weiss IM, Tuross N, Addadi L, Weiner S. 2002. Mollusc larval shell formation: Amorphous  
563 calcium carbonate is a precursor phase for aragonite. *J Exp Zool*. 293(5):478-491.

564 Witte F, Dokas J, Neuendorf F, Mundlos S, Stricker S. 2009. Comprehensive expression  
565 analysis of all wnt genes and their major secreted antagonists during mouse limb  
566 development and cartilage differentiation. *Gene Expr Patterns*. 9(4):215-223.

567 Witten PE, Hall BK. 2003. Seasonal changes in the lower jaw skeleton in male atlantic salmon  
568 (*salmo salar* l.): Remodelling and regression of the kype after spawning. *J Anat*.  
569 203(5):435-450.

570 Zhao M, He M, Huang X, Wang Q. 2014. A homeodomain transcription factor gene, pfmsx,  
571 activates expression of pif gene in the pearl oyster *Pinctada fucata*. *PLoS One*.  
572 9(8):e103830.

573 Zhao M, Shi Y, He M, Huang X, Wang Q. 2016. Pfsmad4 plays a role in biomineralization and  
574 can transduce bone morphogenetic protein-2 signals in the pearl oyster *Pinctada*  
575 *fucata*. *BMC Dev Biol*. 16:9.

576 Zhao R, Takeuchi T, Luo YJ, Ishikawa A, Kobayashi T, Koyanagi R, Villar-Briones A, Yamada  
577 L, Sawada H, Iwanaga S et al. 2018. Dual gene repertoires for larval and adult shells  
578 reveal molecules essential for molluscan shell formation. *Mol Biol Evol*. 35(11):2751-  
579 2761.

580

581

582 **Data Availability**

583 Raw read data generated in this publication is freely available at NCBI SRA with the following  
584 accession PRJNA803976. All analysis scripts and results are available in Supplementary File  
585 1.

586

587 **Acknowledgements and Funding Information**

588 We are grateful to Andrew Gillis for use for paraffin histology and microscopy equipment and  
589 enthusiastic support of this work and the Rothera marine team for collecting the adult *Laternula*  
590 *elliptica* broodstock.

591 This work was supported by UKRI Natural Environment Research Council (NERC) Core  
592 Funding to the British Antarctic Survey, a DTG Studentship (Project Reference:  
593 NE/J500173/1) and a Junior Research Fellowship to VAS from Wolfson College, University of  
594 Cambridge.

595

596 **Author Contributions**

597 **AC** Performed all wet-lab experiments, contributed to imaging, data analysis and  
598 interpretation, and reviewed and edited the manuscript.

599 **MSC** Contributed to supervision of AC, funded the sequencing, contributed to wet-lab  
600 experiments, imaging and data interpretation, reviewed and edited the manuscript.

601 **EH** Conducted all SEM imaging, contributed to data interpretation and reviewed and edited  
602 the manuscript.

603 **LSP** Conducted adult broodstock collection, contributed to wet-lab experiments and data  
604 interpretation, reviewed and edited the manuscript.

605 **VAS** Conceptualized and oversaw the study, supervised AC, contributed to wet-lab  
606 experiments and imaging, conducted all data analysis and interpretation, prepared all figures  
607 and wrote the manuscript.

608

609 **Competing Interests statement**

610 The authors have no competing interests to declare.

611

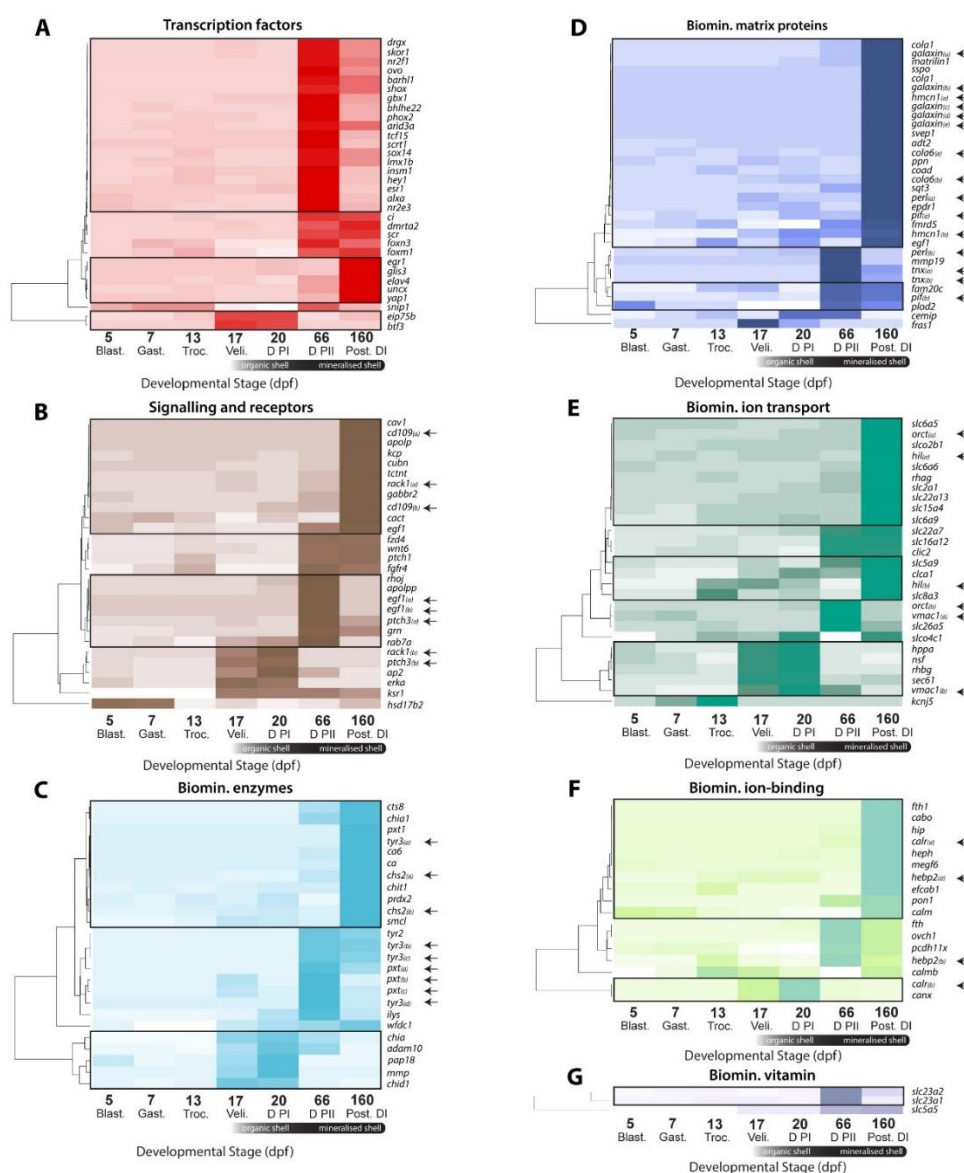
612

613

614

615

616 **Supplementary Figures, Tables and Files**

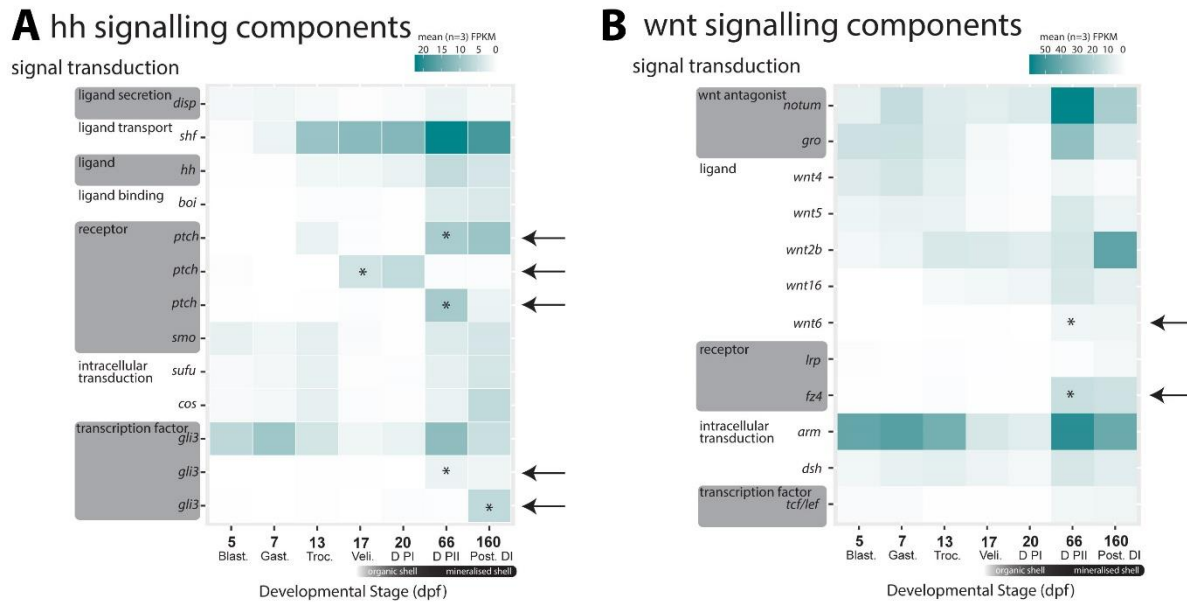


617

618 **Figure S1. Clustered heatplots of significant functionally screened genes from**  
619 **unbiased differential expression analysis, genes typically show stage-specific**  
620 **expression patterns.** Mean average FPKM (n=3) z-scaled over developmental time and  
621 clustered by temporal expression profile on y axis only using hclust (method = single,  
622 clustering represented by dendograms on left). Multiple isoforms of the same gene with  
623 unconfirmed nomenclature labelled with lowercase letters in parentheses and highlighted with  
624 arrows.

625

626



627 **Figure S2. Both hh and wnt signalling pathway genes were significantly upregulated**  
628 **during shell development and could be involved in patterning and proliferation of the**  
629 **larval shell field and larval mantle.** A Heatplot of hh signalling genes and B wnt signalling  
630 **genes. Statistically significantly upregulated genes (edgeR, FDR<0.05, log<sub>2</sub>FC>2) identified**  
631 **with arrows and stage at which significantly upregulated marked with an asterisks (\*).** Order  
632 **of genes on the y axis presented in terms of signal transduction cascades from ligand**  
633 **secretion towards the top and recruitment of downstream transcription factors to the nucleus**  
634 **at the bottom.**

635

636 **Table S1. Summary statistics for *de novo* assembled *Laternula elliptica***  
637 **developmental transcriptome.**

638

639

---

**Reads:**

---

Raw reads	309,593,642
Clean reads	296,480,254
Normalised reads	64,355,068

---

**Assembly:**

---

Total trinity transcripts	964,764
Total trinity genes	666,835
% GC	46.3

---

**Statistics based on all isoforms per gene:**

---

N50	720
Median length	462
Mean average length	662

---

**Read representation (average read content per library):**

---

<b>BUSCO v3, Metazoa Gene Set (n=978)</b>	C:99.1%[S:30%,D:69%] F:0.7%,M:0.2%
---	------------------------------------

---

640 **Supplementary file 1.** Data archive including readme.txt file detailing curation, includes  
641 annotations, statistical analysis R scripts and results tables.

642